Modeling temporal dynamics of genetic diversity in stage-structured plant populations with reference to demographic genetic structure

Yoichi Tsuzuki[a], Takenori Takada[a], Masashi Ohara[a]

[a] *Graduate School of Environmental Science, Hokkaido University, N10W5, Sapporo City, 060-0810, Hokkaido Prefecture, Japan*

Abstract

Predicting temporal dynamics of genetic diversity is important for assessing long-term population persistence. In stage-structured populations, especially in perennial plant species, genetic diversity is often compared among life history stages, such as seedlings, juveniles, and flowerings, using neutral genetic markers. The comparison among stages is sometimes referred to as demographic genetic structure, which has been regarded as a proxy of potential genetic changes because individuals in mature stages will die and be replaced by those in more immature stages over the course of time. However, due to the lack of theoretical examination, the basic property of the stage-wise genetic diversity remained unclear. We developed a matrix model which was made up of difference equations of the probability of non-identical-by-descent of each life history stage at a neutral locus to describe the dynamics and the inter-stage differences of genetic diversity in stage-structured plant populations. Based on the model, we formulated demographic genetic structure as well as the annual change rate of the probability of non-identical-by-descent (denoted as η). We checked if theoretical expectations on demographic ge-

netic structure and η obtained from our model agreed with computational results of stochastic simulation using randomly generated 3,000 life histories. We then examined the relationships of demographic genetic structure with effective population size N_e, which is the determinants of diversity loss per generation time. Theoretical expectations on η and demographic genetic structure fitted well to the results of stochastic simulation, supporting the validity of our model. Demographic genetic structure varied independently of N_e and η, while having a strong correlation with stable stage distribution: genetic diversity was lower in stages with fewer individuals. Our results indicate that demographic genetic structure strongly reflects stable stage distribution, rather than temporal genetic dynamics, and that inferring future genetic diversity solely from demographic genetic structure would be misleading. Instead of demographic genetic structure, we propose η as an useful tool to predict genetic diversity at the same time scale as population dynamics (i.e., per year), facilitating evaluation on population viability from a genetic point of view.

Keywords: effective population size, expected heterozygosity, life history, matrix model, non-identical-by-descent

---

1. Introduction

Genetic diversity, or standing genetic variation, is a source of adaptive evolution (Barrett and Schluter, 2008). Populations with high genetic diversity are more likely to adapt to environmental changes and to persist for a long period (Agashe et al., 2011; Ramsayer et al., 2013). Therefore, it is necessary to examine the temporal dynamics of genetic diversity for assessing

long-term population viability (Mimura et al., 2017).

The rate of change in genetic diversity per generation time is primarily determined by the effective population size (N_e): the larger N_e, the weaker genetic drift, and the more likely genetic diversity is maintained (Crow and Kimura, 1970). Although N_e was first theoretically proposed for populations without generation overlap, many wild populations including perennial plants have overlapping generations and are made up of individuals differing in age or life history stage. Previous theoretical studies extended the concept of effective population size to populations structured by age (Felsenstein, 1971; Hill, 1972, 1979; Johnson, 1977) or by stage (Orive, 1993; Yonezawa et al., 2000) by formulating N_e with demographic rates (age- or stage-specific survival rates and fecundities). These formulations enable us to calculate N_e and to assess the temporal genetic dynamics in species with complex life histories (Waples et al., 2011, 2013).

Meanwhile, some empirical genetic studies do not examine N_e to predict future genetic diversity of stage-structured populations. Instead, genetic diversity is comparatively estimated for each stage class at a single time point with neutral genetic markers (Aldrich et al., 1998; Ally and Ritland, 2006; Kettle et al., 2007; Linhart et al., 1981; Murren, 2003; Schmidt et al., 2018; Vranckx et al., 2014). The resultant stage-wise genetic diversity is sometimes referred to as demographic genetic structure (Aldrich et al., 1998) and is considered to reflect potential genetic changes that accompany the turnover of constituent individuals. For example, if juvenile stage is less diverse than more mature stages, genetic diversity would decrease with the replacement of mature individuals to juveniles. Because species with stage structure are

mostly long-lived and long-term genetic monitoring is impractical, demographic genetic structure has been considered as a rough but a convenient empirical approach to infer the temporal genetic dynamics (Mimura et al., 2017; Schmidt et al., 2018).

Despite its empirical usage, mathematical and theoretical basis of demographic genetic structure has been in its infancy. Unlike N_e, demographic genetic structure has not been formulated mathematically using demographic rates. Relationships with N_e have also remained unexplored, which raises a question on whether N_e and demographic genetic structure are largely redundant or highlight different aspects of temporal genetic dynamics. Moreover, lack of theoretical background draws concerns about the current interpretation on demographic genetic structure. While analysis on demographic genetic structure implicitly assumes that individuals sequentially grow and die from juvenile to mature stage classes, this assumption is potentially invalid in perennial plants. In most perennial plant species, whose life histories are structured by stage, not by age (Silvertown, 1987), aging (or passing of time) does not necessarily promote growth and maturation. Some individuals might keep proceeding to more mature stages, while others remain in the same stage for a long period (stasis) or even reverse to more juvenile stages (retrogression), and the probabilities of growth, stasis, and retrogression depend on stage, rather than on age. For example, long-lived woodland perennial herbs of the genus *Trillium* show stasis for more than ten years in juvenile stages as well as go back from a mature reproductive stage to a pre-reproductive one in response to resource exhaustion (Knight, 2004; Ohara et al., 2001; Tomimatsu and Ohara, 2010). The static and bidirectional flows

in the life cycle complicate the order of individual turnover in a population. It has not been theoretically confirmed if demographic genetic structure still serves as a proxy for temporal changes despite these challenges. Mathematical formulation that encompasses demographic genetic structure, as well as the temporal change in genetic diversity, will provide integrative understandings on all the problems mentioned above in stage-structured populations, but has never been achieved so far.

In this study, we develop a matrix model to describe the temporal dynamics of genetic diversity for a neutral locus of a stage-structured perennial plant species. The model is constructed by deriving difference equations of the probability that two genes randomly sampled from a given life history stage are non-identical-by-descent. Based on the model, we formulate demographic genetic structure and N_e. Thus, our model allows integrative analysis on demographic genetic structure, temporal dynamics of genetic diversity, and their relationships. In the following sections, we describe the derivation procedures of our model (section 2.1), the validation of our model (section 2.2), and the assessment on whether demographic genetic structure serves as a good proxy for the temporal changes in genetic diversity (section 2.3).

2. Materials and Methods

2.1. Model development

2.1.1. Overview

Felsenstein (1971) derived inbreeding effective population size for age-structured populations by formulating recurrence equations of the probability

of non-identical-by-descent, which is also described in Charlesworth (1994). We partly follow mathematical formulation procedures in Felsenstein (1971) while adding necessary modifications to extend it to stage-structured populations. We develop difference equations of the probability of non-identical-by-descent at a neutral locus for a closed, stage-structured population, supposing a diploid perennial plant species. We do not consider sex differences because most plants are hermaphrodite (Torices et al., 2011). We assume that mutations do not newly occur. Besides, as in Felsenstein (1971), we assume demographic equilibrium, where the census population size and its allocation to each stage (stage distribution) are constant over time. Census population size is set to N, which is divided into n life history stages $(N_1, N_2, \cdots, N_n)$.

$$N = \sum_{i=1}^{n} N_i \tag{1}$$

The probability of transition (either growth, stasis, or retrogression) from stage j to stage i is t_{ij} per year. In each year, individuals randomly mate and f_{ij} newborns join stage i from a parent in stage j. a_{ij}, which denotes the sum of t_{ij} and f_{ij}, describes the total flow of individuals from stage j to i between successive years.

$$a_{ij} = t_{ij} + f_{ij}. \tag{2}$$

In age-structured life histories, flows of individuals among age classes are sparse: survival paths connect only adjacent ages in the direction from i to $i+1$ (i.e., $t_{ij} = 0$ when $i \neq j+1$), and reproduction paths join only age class 1 (i.e., $f_{ij} = 0$ when $i \neq 1$). In plants, however, multiple survival paths come in and out from each stage by the combination of growth, stasis, and

retrogression. Moreover, newborns do not always join the first stage, because newborn seeds either become dormant to join seed bank stage, or immediately germinate to join juvenile stages, resulting in multiple destinations (e.g., a perennial plant *Carduus nutans*, whose life cycle is shown in figure 1 of Shea and Kelly (1998)). Therefore, stage is not merely a pooling of successive age classes and stage-structured life histories are essentially different from age-structured ones. We need to consider all possible transition and reproduction paths among stages, which is quite a distinct point compared to the age-structured model in Felsenstein (1971).

Population dynamics can be modeled by the following matrix population model.

$$\begin{pmatrix} N_{1,t} \\ \vdots \\ N_{i,t} \\ \vdots \\ N_{n,t} \end{pmatrix} = \begin{pmatrix} a_{11} & \cdots & a_{1j} & \cdots & a_{1n} \\ \vdots & & \vdots & & \vdots \\ a_{i1} & \cdots & a_{ij} & \cdots & a_{in} \\ \vdots & & \vdots & & \vdots \\ a_{n1} & \cdots & a_{nj} & \cdots & a_{nn} \end{pmatrix} \begin{pmatrix} N_{1,t-1} \\ \vdots \\ N_{i,t-1} \\ \vdots \\ N_{n,t-1} \end{pmatrix}. \tag{3}$$

$N_{i,t}$ denotes the number of individuals in stage i in year t, which is always equal to N_i for any t because we assume demographic equilibrium. Stable stage distribution, which is the relative number of individuals among stages in the equilibrium state, is proportional to the leading right eigenvector of the transition matrix (Caswell, 2001).

We define $H_{ij,t}$ as the probability that two genes randomly sampled from stage i and j with replacement in year t are not identical-by-descent. Each gene has its own ancestry, and two-gene pairs that are (non-)identical-by-descent at $t = 0$ will remain the same for any t. Similarly, because we assume

no mutations, two-gene pairs that are (non-)identical-by-state at $t = 0$ will also remain the same over time. This means that $H_{ij,t}$ behaves in the same manner as expected heterozygosity, which is the probability of non-identical-by-state and is commonly used as a proxy of genetic diversity. Our goal is to formulate $H_{ij,t}$ for all possible i and j, which enables us to obtain theoretical counterpart of demographic genetic structure, that is, stage-wise genetic diversity at a particular time point.

Here, we provide key derivation procedures, highlighting the differences with the preceding age-structured models in Felsenstein (1971). The complete derivation procedures are given in Supporting Information 1.

2.1.2. Difference equations of $H_{ij,t}$

We begin with modeling the changes in $H_{ij,t}$ between two successive time points for all i and j, which are the stage-structured version of equations 2 to 5 in Felsenstein (1971). We separately consider two mutually exclusive situations: $i \neq j$ (case 1) and $i = j$ (case 2). Both cases can be further split into six situations. Firstly, two genes randomly sampled in year t were either in the same stage (say, stage m, case A) or in different stages (say, stage k and l, case B) in year $t - 1$. Furthermore, genes can move among stages either by survival (grow, stasis, and retrogression) or by reproduction. Survival and reproduction are essentially different because reproduction allows one gene to be replicated and to move to multiple stages simultaneously and independently, while survival does not. There are three possibilities in how the two genes sampled were transferred from the previous year: both genes were transferred by survival (case α), one by survival and the other by reproduction (case β), and both by reproduction (case γ). Considering

148 the combinations of where (case A and B) and how (case α, β, and γ) the
149 two genes sampled came from, there are 6 mutually exclusive situations to
150 be considered in both case 1 and 2 (Figure 1).

151 This classification scheme is original to our stage-structured model, and is
152 not adopted in Felsenstein (1971). Compared to age-structured life histories,
153 classes are more densely interconnected by survival and reproduction in stage-
154 structured ones. It is necessary to consider as many as 12 situations to handle
155 the complexity in plant life histories.

156 In case 1 (i.e., $i \neq j$), $H_{ij,t}$ can be decomposed as follows.

$$\begin{aligned} H_{ij,t} =& H_{ij,t}|_{1\cap A\cap\alpha} + H_{ij,t}|_{1\cap A\cap\beta} + H_{ij,t}|_{1\cap A\cap\gamma} \\ &+ H_{ij,t}|_{1\cap B\cap\alpha} + H_{ij,t}|_{1\cap B\cap\beta} + H_{ij,t}|_{1\cap B\cap\gamma}, \end{aligned} \tag{4}$$

157 where the cap symbol $\cap$ stands for the co-occurrence of multiple cases:
158 $H_{ij,t}|_{1\cap Y\cap Z}$ stands for $H_{ij,t}$ that simultaneously satisfies case 1, Y, and Z
159 ($Y = A, B$; $Z = \alpha, \beta, \gamma$). All six $H_{ij,t}|_{1\cap Y\cap Z}$ on the right side of equation 4
160 are formulated as follows (see Supporting Information 1.1 for details).

$$H_{ij,t}|_{1\cap A\cap\alpha} = \sum_{m=1}^{n} \left\{ \frac{t_{im}t_{jm}N_m^2}{N_iN_j} \times \frac{1}{1-1/(2N_m)} H_{mm,t-1} \right\}$$

$$H_{ij,t}|_{1\cap A\cap\beta} = \sum_{m=1}^{n} \left\{ \frac{(t_{im}f_{jm}+f_{im}t_{jm})N_m^2}{N_iN_j} \times H_{mm,t-1} \right\}$$

$$H_{ij,t}|_{1\cap A\cap\gamma} = \sum_{m=1}^{n} \left(\frac{f_{im}f_{jm}N_m^2}{N_iN_j} \times H_{mm,t-1} \right)$$

$$H_{ij,t}|_{1\cap B\cap\alpha} = \sum_{k=1}^{n} \sum_{\substack{l=1 \\ l\neq k}}^{n} \left\{ \frac{(t_{ik}t_{jl}+t_{il}t_{jk})N_kN_l}{N_iN_j} \times H_{kl,t-1} \right\}$$

$$H_{ij,t}|_{1\cap B\cap\beta} = \sum_{k=1}^{n} \sum_{\substack{l=1 \\ l\neq k}}^{n} \left\{ \frac{(t_{ik}f_{jl}+f_{ik}t_{jl}+t_{il}f_{jk}+f_{il}t_{jk})N_kN_l}{N_iN_j} \times H_{kl,t-1} \right\}$$

$$H_{ij,t}|_{1\cap B\cap\gamma} = \sum_{k=1}^{n}\sum_{\substack{l=1\\ l\neq k}}^{n}\left\{\frac{(f_{ik}f_{jl}+f_{il}f_{jk})N_kN_l}{N_iN_j}\times H_{kl,t-1}\right\}. \quad (5)$$

Each $H_{ij,t}|_{1\cap Y\cap Z}$ is shown as a summation of a multiplications of two terms. The first term is a conditional probability of case $1\cap Y\cap Z$ given case 1. For example, the first term of $H_{ij,t}|_{1\cap A\cap\alpha}$ can be rewritten as $(2t_{im}N_m)/(2N_i)\times(2t_{jm}N_m)/(2N_j)$, which is the number of two-gene pairs that fall into case 1, A, and α simultaneously under a specific m (i.e., $2t_{im}N_m\times 2t_{jm}N_m$) divided by the total number of pairs that satisfy case 1 (i.e., $2N_i\times 2N_j$). Here, the number of genes are twice the number of individuals because we assume diploid species. Similarly, the first term in the other five equations stand for the corresponding proportion of two-genes pairs. The second term stands for the probability of non-identical-by-descent. Considering which stages the two genes sampled belonged to in year $t-1$, we replace the probability with either $H_{mm,t-1}$ or $H_{kl,t-1}$, except $H_{ij,t}|_{1\cap A\cap\alpha}$. In the case of $1\cap A\cap\alpha$, genes sampled from stage i must be mutually exclusive against those from stage j, because one gene in stage m in year $t-1$ could not move to both stage i and j simultaneously without being duplicated through reproduction. In other words, a gene that were in stage m in the previous year cannot be sampled twice, which violates the assumption of $H_{mm,t-1}$, that is, "sampling with replacement." Therefore, $H_{ij,t}|_{1\cap A\cap\alpha}$ inherits the probability that two genes randomly sampled from stage m "without" replacement in year $t-1$ were not identical-by-descent, which can be obtained by dividing $H_{mm,t-1}$ by the chance of not sampling the same gene twice $(=1-1/(2N_m))$.

Substituting equations 5 to equation 4, $H_{ij,t}$ is formulated as follows.

$$H_{ij,t} = \sum_{m=1}^{n} \frac{N_m^2}{N_i N_j} \left\{ \frac{t_{im} t_{jm}}{1 - 1/(2N_m)} + f_{im} t_{jm} + t_{im} f_{jm} + f_{im} f_{jm} \right\} H_{mm,t-1} + \sum_{k=1}^{n} \sum_{\substack{l=1 \\ l \neq k}}^{n} \frac{N_k N_l}{N_i N_j} (a_{ik} a_{jl} + a_{il} a_{jk}) H_{kl,t-1}. \quad (6)$$

As for case 2 (i.e., $i = j$), we decompose $H_{ii,t}$ into six conditional probabilities.

$$H_{ii,t} = H_{ii,t}|_{2 \cap A \cap \alpha} + H_{ii,t}|_{2 \cap A \cap \beta} + H_{ii,t}|_{2 \cap A \cap \gamma} + H_{ii,t}|_{2 \cap B \cap \alpha} + H_{ii,t}|_{2 \cap B \cap \beta} + H_{ii,t}|_{2 \cap B \cap \gamma}. \quad (7)$$

The probabilities of non-identical-by-descent on the right side of equation 7 can be formulated with $H_{mm,t-1}$ and $H_{kl,t-1}$, as previously done for $H_{ij,t}$ in case 1 (see Supporting Information 1.2 for details).

$$\begin{aligned}
H_{ii,t}|_{2 \cap A \cap \alpha} &= \sum_{m=1}^{n} \left\{ \left(\frac{t_{im} N_m}{N_i} \right)^2 \times \frac{1 - 1/(2 t_{im} N_m)}{1 - 1/(2N_m)} H_{mm,t-1} \right\} \\
H_{ii,t}|_{2 \cap A \cap \beta} &= \sum_{m=1}^{n} \left(\frac{2 t_{im} f_{im} N_m^2}{N_i^2} \times H_{mm,t-1} \right) \\
H_{ii,t}|_{2 \cap A \cap \gamma} &= \sum_{m=1}^{n} \left\{ \left(\frac{f_{im} N_m}{N_i} \right)^2 \times \left(1 - \frac{1}{2 f_{im} N_m} \right) H_{mm,t-1} \right\} \\
H_{ii,t}|_{2 \cap B \cap \alpha} &= \sum_{k=1}^{n} \sum_{\substack{l=1 \\ l \neq k}}^{n} \left(\frac{2 t_{ik} t_{il} N_k N_l}{N_i^2} \times H_{kl,t-1} \right) \\
H_{ii,t}|_{2 \cap B \cap \beta} &= \sum_{k=1}^{n} \sum_{\substack{l=1 \\ l \neq k}}^{n} \left\{ \frac{2 (t_{ik} f_{il} + f_{ik} t_{il}) N_k N_l}{N_i^2} \times H_{kl,t-1} \right\} \\
H_{ii,t}|_{2 \cap B \cap \gamma} &= \sum_{k=1}^{n} \sum_{\substack{l=1 \\ l \neq k}}^{n} \left(\frac{2 f_{ik} f_{il} N_k N_l}{N_i^2} \times H_{kl,t-1} \right).
\end{aligned} \quad (8)$$

Here, as with $H_{ij,t}|_{1\cap A\cap\alpha}$ in case 1, the second term of $H_{ii,t}|_{2\cap A\cap\alpha}$ and $H_{ii,t}|_{2\cap A\cap\gamma}$ are not exactly the same as $H_{mm,t-1}$. This is because the sources from which two genes are sampled cannot be replaced with stage m of the previous year. Case $2\cap A\cap\alpha$ and $2\cap A\cap\gamma$ are the same situations as the case of "$i = j > 1$" and "$i = j = 1$" of the age-structured model in Felsenstein (1971), respectively. Therefore, we followed Felsenstein (1971) to adjust $H_{mm,t-1}$ by multiplying $(1-1/(2t_{im}N_m))/(1-1/(2N_m))$ and $1-1/(2f_{im}N_m)$ in case $2\cap A\cap\alpha$ and $2\cap A\cap\gamma$. Improving the explanation of Felsenstein (1971) to fit to our stage-structured model, We give detailed procedures on the adjustment of $H_{mm,t-1}$ in Supporting Information 1.2.

Substituting equations 8 to equation 7, $H_{ii,t}$ is formulated as follows.

$$H_{ii,t} = \sum_{m=1}^{n} \left\{ \left(\frac{t_{im}N_m}{N_i} \right)^2 \frac{1-1/(2t_{im}N_m)}{1-1/(2N_m)} + \frac{2t_{im}f_{im}N_m^2}{N_i^2} + \left(\frac{f_{im}N_m}{N_i} \right)^2 \left(1 - \frac{1}{2f_{im}N_m} \right) \right\} H_{mm,t-1} + \sum_{k=1}^{n} \sum_{\substack{l=1 \\ l\neq k}}^{n} \frac{2a_{ik}a_{il}N_kN_l}{N_i^2} H_{kl,t-1}. \quad (9)$$

Combining case 1 (equation 6) and 2 (equation 9), we construct a matrix equation.

$$\boldsymbol{h_t} = \boldsymbol{M}\boldsymbol{h_{t-1}}. \quad (10)$$

$\boldsymbol{h_t}$ and $\boldsymbol{h_{t-1}}$ are vectors, each of which consists of $H_{ij,t}$ and $H_{ij,t-1}$ for all possible pairs of i and j ($1 \leq i \leq n$, $1 \leq j \leq n$). As the number of two-stage pairs is $n(n+1)/2$, both $\boldsymbol{h_t}$ and $\boldsymbol{h_{t-1}}$ have $n(n+1)/2$ elements. $\boldsymbol{M}$ is a square matrix whose dimension is $n(n+1)/2$ and whose elements are equal to the corresponding coefficients of $H_{mm,t-1}$ and $H_{kl,t-1}$ in equations 6 and 9

(see Supporting Information 2 for the detailed elements of $\boldsymbol{M}$). The order of elements in $\boldsymbol{h_t}$ is arbitrary as long as it matches with that in $\boldsymbol{h_{t-1}}$ and $\boldsymbol{M}$.

In general, multiplying matrix $\boldsymbol{M}$ is asymptotically the same as multiplying the dominant eigenvalue of $\boldsymbol{M}$, while $\boldsymbol{h_t}$ converges to a scalar multiplication of the leading right eigenvector, for sufficiently large t.

$$\boldsymbol{h_t} = \eta \boldsymbol{h_{t-1}}, \tag{11}$$

$$\boldsymbol{h_t} \propto \boldsymbol{w}, \tag{12}$$

where η and $\boldsymbol{w}$ are the leading eigenvalue and its corresponding right eigenvector of matrix $\boldsymbol{M}$, respectively. We denote w_{ij} as the element of $\boldsymbol{w}$ that corresponds to $H_{ij,t}$ of $\boldsymbol{h_t}$.

$$H_{ij,t} \propto w_{ij}. \tag{13}$$

Equation 11 means that $H_{ij,t}$ changes with a constant rate η over the course of time for all i and j. Here, we denote H_t as the probability of non-identical-by-descent of the whole population in time t. H_t can be formulated as the sum of $H_{ij,t}$ weighted by the number of individuals in stage i and j.

$$H_t = \sum_{i=1}^{n} \sum_{j=1}^{n} \frac{N_i N_j}{N^2} H_{ij,t} \propto \sum_{i=1}^{n} \sum_{j=1}^{n} \frac{N_i N_j}{N^2} w_{ij}. \tag{14}$$

Because we assume that population size (N) and the number of individuals in a given stage i (N_i) are constant, H_t changes with the same rate as $H_{ij,t}$, that is, η.

$$H_t = \eta H_{t-1}. \tag{15}$$

Felsenstein (1971) also reached an analogous conclusion in his age-structured model that $H_{ij,t}$ and the probability of non-identical-by-descent of the overall population changed at the same rate, which was the largest eigenvalue.

However, the proportionality between the array of $H_{ij,t}$ and the leading right eigenvector $\boldsymbol{w}$, which is shown in equations 12 and 13, was not mentioned in Felsenstein (1971).

2.1.3. Demographic genetic structure

We use the logarithm of the ratio of $H_{ii,t}$ between different stages as a proxy of demographic genetic structure, that is, comparison of genetic diversity among stages. With regard to the comparison between stage i and j, the logarithmic ratio is formulated as follows, based on equation 13.

$$\log\left(\frac{H_{ii,t}}{H_{jj,t}}\right) = \log\left(\frac{w_{ii}}{w_{jj}}\right), \tag{16}$$

When $\log(H_{ii,t}/H_{jj,t})$ is positive, $H_{ii,t}$ is larger than $H_{jj,t}$ (genetic diversity is higher in stage i than in stage j), and when negative vice versa. It should be noted that $\log(H_{ii,t}/H_{jj,t})$ is time-invariant, although $H_{ii,t}$ and $H_{jj,t}$ themselves change with time.

We formulate inter-stage genetic differentiation as an extra extension of our model. While genetic differentiation has not been examined as much as to the difference in genetic diversity has, it is another aspect of stage-wise genetic structure. By denoting $\overline{H}_{ii,t}$ and $\overline{w}_{ii}$ as the arithmetic mean of $H_{ii,t}$ for all i and as that of corresponding elements in $\boldsymbol{w}$, respectively, we define inter-stage F_{st} as follows.

$$F_{st} = \frac{H_t - \overline{H}_{ii,t}}{H_t} = 1 - \frac{\overline{w_{ii}}N^2}{\sum_i \sum_j w_{ij} N_i N_j}. \tag{17}$$

We use equations 13 and 14 to derive the rightmost-side of equation 17. It should be noted that F_{st} is also time-invariant, as with $\log(H_{ii,t}/H_{jj,t})$.

2.1.4. Effective population size

As in Felsenstein (1971), we formulate effective population size N_e using the dominant eigenvalue η. The probability of non-identical-by-descent of the overall population decreases with the rate of $1/(2N_e)$ per generation time (Crow and Kimura, 1970).

$$H_{t+T} = \left(1 - \frac{1}{2N_e}\right) H_t, \tag{18}$$

where T is generation time and is defined as the mean age of net fecundity in the cohort (Carey & Roach, 2020, see Supporting Information 1.3 for details). Considering that H_t changes with the rate of η per year (equation 15), $1 - 1/(2N_e)$ should be equivalent to η^T. Therefore, We formulate N_e as follows.

$$N_e = \frac{1}{2(1 - \eta^T)} \tag{19}$$

To sum up, demographic genetic structure and effective population size are derived from the leading right eigenvector and from the dominant eigenvalue of matrix $\boldsymbol{M}$, respectively. Therefore, our matrix model integrates the two proxies of the temporal genetic dynamics, facilitating comprehensive understandings on demographic genetic structure.

2.2. Validation of the model

To ensure that our model was formulated adequately, we compared theoretically obtained η and demographic genetic structure with observed ones computed by stochastic simulation. We arranged a set of life histories to be used for the comparison between theory and simulation. We considered perennial plants with two ($n = 2$: juvenile and adult) and three stages ($n = 3$:

seed, juvenile, and adult; Figure 2). Equation 10 can be rewritten as follows.

$$\begin{pmatrix} H_{11,t} \\ H_{22,t} \\ H_{12,t} \end{pmatrix} = \boldsymbol{M_2} \begin{pmatrix} H_{11,t-1} \\ H_{22,t-1} \\ H_{12,t-1} \end{pmatrix}, \tag{20}$$

and

$$\begin{pmatrix} H_{11,t} \\ H_{22,t} \\ H_{33,t} \\ H_{12,t} \\ H_{23,t} \\ H_{13,t} \end{pmatrix} = \boldsymbol{M_3} \begin{pmatrix} H_{11,t-1} \\ H_{22,t-1} \\ H_{33,t-1} \\ H_{12,t-1} \\ H_{23,t-1} \\ H_{13,t-1} \end{pmatrix}. \tag{21}$$

Equation 20 and 21 correspond to the case of $n = 2$ and $n = 3$, respectively. The elements of $\boldsymbol{M_2}$ and $\boldsymbol{M_3}$ are functions of demographic rates (t_{ij}, f_{ij}) and the number of individuals in each stage (N_i, see Supporting Information 2 for details). For each of the two- and the three-stage model, we randomly generated five hundreds life histories which differed in t_{ij}, f_{ij}, and N_j, covering a wide range of life history strategies (Figure S1). We indirectly determined parameter values of t_{ij}, f_{ij}, and N_j. Firstly, the total population size N was set to 100, and then N was randomly divided into all possible survival and reproduction paths (i.e., $t_{ij}N_j$ and $f_{ij}N_j$). In the case of the two-stage model, for example, 100 individuals were randomly split into five paths: stasis at juvenile, growth from juvenile to adult, retrogression from adult to juvenile, stasis at adult, and reproduction (Figure 2a). Next, N_i was calculated by $\sum_{i=1}^{n}(t_{ij}N_j + f_{ij}N_j)$, and finally t_{ij} and f_{ij} were calculated by $t_{ij}N_j/N_j$ and $f_{ij}N_j/N_j$ respectively (see Supporting Information 3 for details). By deter-

mining $t_{ij}N_j$ and $f_{ij}N_j$ first, we could easily search the parameter space while keeping the number of individuals (i.e., N_i, $t_{ij}N_j$, and $f_{ij}N_j$ for all i and j) to be always integer. To consider the situation of $N = 500$ and $N = 1,000$, we multiplied N_1 and N_2 (when $n = 3$, N_3 as well) by 5 and 10 while keeping demographic rates unchanged. In total, we considered 1,500 sets of parameter values (500 sets of demographic rates $\times$ 3 sets of N) for each of the two- and the three-stage model.

For each parameter set, we simulated 200 years of temporal dynamics of expected heterozygosity at a neutral biallelic locus 100 times. We calculated the mean expected heterozygosity over the 100 replicates for the overall population and for all the two-stage pairs at every t, which were denoted as $\hat{H}_t$ and $\hat{H}_{ij,t}$, respectively. All simulations were initiated with maximum expected heterozygosity, in which two alleles share the gene pool half-and-half in all stages (i.e., $H_0 = H_{ij,0} = 0.5$ for all i and j). It should be noted that the initial state of equal gene frequencies among classes corresponds to a genetic equilibrium under no evolutionary forces (i.e., drift, selection, mutation and gene flow) (Charlesworth, 1994). Therefore, it could be said that our simulation results reflected how genetic drift solely decreased genetic diversity in stage-structured populations.

We calculated the annual change rate of $\hat{H}_t$ by

$$r_t = \frac{\hat{H}_t}{\hat{H}_{t-1}}, \tag{22}$$

where $1 \leq t \leq 200$. We took logarithm of r_t and calculated its mean and standard error, which were subsequently compared to η. η is the theoretical counterpart r_t and was obtained as the dominant eigenvalue of matrix $\boldsymbol{M_2}$ or $\boldsymbol{M_3}$.

Using simulation results, we also calculated the mean of demographic genetic structure over the 200 years. As for the two-stage model, we calculated $\log(\hat{H}_{11,t}/\hat{H}_{22,t})$. We calculated $\log(\hat{H}_{11,t}/\hat{H}_{22,t})$, $\log(\hat{H}_{22,t}/\hat{H}_{33,t})$ and $\log(\hat{H}_{11,t}/\hat{H}_{33,t})$ in the case of the three-stage model. These four proxies of observed demographic genetic structures were compared to theoretical counterparts, that is, $\log(H_{11,t}/H_{22,t})$ for the two-stage model, as well as $\log(H_{11,t}/H_{22,t})$, $\log(H_{22,t}/H_{33,t})$ and $\log(H_{11,t}/H_{33,t})$ for the three-stage model. These four logarithmic ratios were obtained by solving the leading right eigenvector of $\boldsymbol{M_2}$ and $\boldsymbol{M_3}$ and substituting their elements to equation 16.

2.3. Analysis on demographic genetic structure

For the same 3,000 parameter sets as "Validation of the model" section, we analytically obtained η and N_e, which reflect the change rate of all $H_{ij,t}$ per year and per generation, respectively. η was obtained by solving the dominant eigenvalue of $\boldsymbol{M_2}$ and $\boldsymbol{M_3}$. Then, using η, we obtained N_e based on equation 19. We examined if η and N_e, both of which genuinely represent temporal dynamics of genetic diversity, were correlated with the four logarithmic ratios that stood for demographic genetic structure (i.e., $\log(H_{11,t}/H_{22,t})$ for the two-stage model, and $\log(H_{11,t}/H_{22,t})$, $\log(H_{22,t}/H_{33,t})$ and $\log(H_{11,t}/H_{33,t})$ for the three-stage model) to judge if demographic genetic structure could serve as a proxy for temporal dynamics of genetic diversity across a wide range of life history strategies.

Moreover, to explore basic behaviors of demographic genetic structure, we analyzed the dependence of demographic genetic structure on total population size N and stable stage distribution. Stable stage distribution was quantified by the logarithm of the ratio among N_1, N_2, and N_3 (i.e., $\log(N_1/N_2)$,

$\log(N_2/N_3)$, and $\log(N_1/N_3)$).

3. Results

3.1. Validation of the model

The rate of change in expected heterozygosity of the overall populations (r_t), which was computed by simulation, took almost exactly the same value as the theoretical counterpart η for all 1,500 sets of parameter values in both the two- and the three-stage models (Figure 3, S2).

Comparison of demographic genetic structure between simulation and analytical results revealed that our theoretical model yielded almost equivalent logarithmic ratio of expected heterozygosity among stages to that of simulation (Figure 4, S3, S4).

To further confirm the validity of our model, we checked the temporal dynamics of $\hat{H}_{ij,t}$ and compared it with theoretical expectation, that is, the repeated multiplication of matrix $\boldsymbol{M_2}$ or $\boldsymbol{M_3}$ to $\boldsymbol{h_t}$. We found that theoretical prediction fitted well to simulation results (Figure S5).

Thus, our model seems to describe the dynamics and the inter-stage ratio of expected heterozygosity validly across a wide range of parameter space.

3.2. Analysis on demographic genetic structure

All the four proxies of demographic genetic structure, which are theoretically obtained based on equation 16, have an apparent correlation neither with N_e nor with η regardless of N (Figure 5, S6-10). On the other hand, demographic genetic structure is clearly associated with total population size N. As N increases, all the four logarithmic ratios gradually converge

to zero, which means that expected heterozygosity becomes equal among stages (Figure 6). Moreover, there is a strong positive correlation with stable stage distribution: expected heterozygosity is higher in stages with more individuals (Figure 7). The correlation becomes weaker with increasing N, as logarithmic ratios converge to zero.

4. Discussion

4.1. Comparison with the age-structured model

In this study, we develop the matrix model that describes the dynamics of genetic diversity and demographic genetic structure in stage-structured populations. Although the procedures of model development are similar to the age-structured model in Felsenstein (1971), our model has a much wider applicability. First of all, because age-structured models, in which the probabilities of stasis and retrogression are zero, is a special case of stage-structured models, our model is more comprehensive. Besides, many plant species do not show demographic senescence (Jones et al., 2014), showing no age-dependent changes in demographic rates. Using stage-dependent demographic parameters would be more appropriate and predictive in plant populations. These points support the novelty of our stage-structured model, especially in terms of expanding the applicability to many plant species.

4.2. Interpreting demographic genetic structure

A common interpretation on demographic genetic structure is that if juvenile stages are less diverse than mature stages, genetic diversity would decrease with time over the course of generation turnover (Aldrich et al.,

1998; Ally and Ritland, 2006; Kettle et al., 2007; Linhart et al., 1981; Murren, 2003; Schmidt et al., 2018; Vranckx et al., 2014). However, our model shows that relative ratio of expected heterozygosity between stage classes does not correlate with either N_e or η: even though N_e and η are small, expected heterozygosity does not necessarily decline from mature to juvenile stages. Therefore, inferring temporal trends in genetic diversity solely from demographic genetic structure is potentially misleading. This study, to our knowledge, for the first time draws caution on the conventional use of demographic genetic structure.

Many previous empirical studies that analyzed demographic genetic structure found that genetic diversity did not decrease from the most mature to the most immature stages and took comparable values among stages (Aldrich et al., 1998; Ally and Ritland, 2006; Kettle et al., 2007; Linhart et al., 1981; Murren, 2003; Schmidt et al., 2018; Vranckx et al., 2014). Our model shows that the logarithmic ratio of expected heterozygosity is distributed around zero, especially under large N, indicating that expected heterozygosity is basically almost equivalent to one another. Therefore, our model might be in line with previous empirical results.

While demographic genetic structure is irrelevant to temporal dynamics, it is tightly linked to stable stage distribution: expected heterozygosity is relatively high in stage with more individuals, and low in stage with less individuals (Figure 6). In general, small number of individuals intensifies stochastic genetic drift due to increased sampling bias in gene frequencies, leading to the loss of genetic diversity (Crow and Kimura, 1970). When stage distribution is skewed, the degree of stochasticity will vary among stages.

Stage with smaller number of individuals is made up of genes that were sampled fewer times from the gene pool of the previous year, thus suffering random perturbation in gene frequencies to a greater extent. The alleviated stochasticity must have resulted in the lower genetic diversity in stages with fewer individuals.

As the total population size N increases, inter-stage difference in genetic diversity disappears even under the skewed stage distribution (Figure 7). This result indicates that the number of individuals of each stage is large enough to reduce stochasticity under large N, leading to comparable level of genetic diversity among stages. Large population size also contributes to the maintenance of genetic diversity, because N_e increases and η approaches to 1 with increasing N (Figure S11).

To sum up, it can be said that genetic diversity becomes uneven among life history stages under small population size and that the unevenness among stages reflects stable stage distribution rather than the temporal dynamics of genetic diversity.

4.3. Future application of our model

Our model not only provides theoretical background of demographic genetic structure, but also has some potential for application. One possible application is to compare raw demographic genetic structure, which is obtained by any neutral genetic markers, with the theoretical expectation calculated based on the equations we derived. The deviations of observed structure from expectation reflect factors unexplored in our model, such as fluctuating population size, non-random mating, selection, and immigration. Thus, our model can work as a null model of demographic genetic structure. To make

426 the most use of our equations, it is necessary to monitor individuals from year
427 to year to estimate demographic rates of each stage class. If long-term demo-
428 graphic monitoring is unavailable or impractical for some reasons, recording
429 relative number of individuals among stage classes at a single time point
430 would be at least desirable to consider stage distribution, which turned out
431 to be a major determinant of demographic genetic structure in our model.
432 Instead of demographic genetic structure, we want to pay attention to
433 the efficacy of η, which is the annual change rate of the probability of non-
434 identical-by-descent and represents the dynamics of expected heterozygosity
435 well. η can be potentially useful for population viability assessment. Whether
436 population size can be maintained over time (i.e., population growth rate
437 remains high) is considered as a criterion of long-term population persistence
438 (Hens et al., 2017; Knight et al., 2009). Demographic rates have been used to
439 calculate population growth rate per year (usually denoted as λ) by solving
440 the eigenvalue problem of matrix population models (equation 3) (Caswell,
441 2001; Crone et al., 2011). While it is acknowledged that not only population
442 size but also genetic diversity should be maintained for long-term population
443 persistence, there has been no counterpart of population growth rate that
444 can evaluate the change rate of genetic diversity per year (not per generation
445 time). Being a change rate per year, η is directly linked to temporal change
446 in genetic diversity compared to demographic genetic structure and effective
447 population size, and enables us to assess genetic diversity at the same time
448 scale as population dynamics. Therefore, η can serve as the counterpart of
449 λ and can be an useful proxy to evaluate population viability from genetic
450 point of view. It should be noted that we evaluated expected heterozygosity

using the probability of non-identical-by-descent in our model. Because this replacement is based on the assumption of no mutation, our results should be applied to a prediction on a time scale, in which *de novo* mutations do not spread throughout the overall population. Evaluating η for a variety types of structured populations will be a future step to make the best use of our model.

Acknowledgements

This research was financially supported by Grands-in-Aid for Scientific Research from the JSPS KAKENHI (Grant no. 19H03294, 20K06821, and 21J10814).

Declaration of Competing Interest

The authors declare no competing interest.

Author Contributions

Yoichi Tsuzuki: Conceptualization, Methodology, Investigation, Writing - original draft. **Takenori Takada**: Investigation, Writing - review & editing. **Masashi Ohara**: Writing - review & editing.

References

Agashe, D., Falk, J.J., Bolnick, D.I., 2011. Effects of founding genetic variation on adaptation to a novel resource. Evolution 65, 2481–2491. doi:10.1111/j.1558-5646.2011.01307.x.

471 Aldrich, P.R., Hamrick, J.L., Chavarriaga, P., Kochert, G., 1998. Microsatel-
472 lite analysis of demographic genetic structure in fragmented populations
473 of the tropical tree *Symphonia globulifera*. Molecular Ecology 7, 933–944.
474 doi:10.1046/j.1365-294x.1998.00396.x.

475 Ally, D., Ritland, K., 2006. A case study: Looking at the effects of frag-
476 mentation on genetic structure in different life history stages of old-growth
477 mountain hemlock (*Tsuga mertensiana*). Journal of Heredity 98, 73–78.
478 doi:10.1093/jhered/esl048.

479 Barrett, R.D., Schluter, D., 2008. Adaptation from standing ge-
480 netic variation. Trends in Ecology & Evolution 23, 38–44.
481 doi:10.1016/j.tree.2007.09.008.

482 Caswell, H., 2001. Matrix population models. 2 ed., Sinauer Associates, Inc.

483 Charlesworth, B., 1994. Evolution in Age-Structured Populations. 2 ed.,
484 Cambridge University Press.

485 Crone, E.E., Menges, E.S., Ellis, M.M., Bell, T., Bierzychudek, P., Ehrlén,
486 J., Kaye, T.N., Knight, T.M., Lesica, P., Morris, W.F., Oostermeijer, G.,
487 Quintana-Ascencio, P.F., Stanley, A., Ticktin, T., Valverde, T., Williams,
488 J.L., 2011. How do plant ecologists use matrix population models? Ecology
489 Letters 14, 1–8. doi:10.1111/j.1461-0248.2010.01540.x.

490 Crow, J., Kimura, M., 1970. An Introduction to Population Genetics Theory.
491 Harper and Row.

492 Felsenstein, J., 1971. Inbreeding and variance effective numbers in

populations with overlapping generations. Genetics 68, 581–597. doi:10.1093/genetics/68.4.581.

Hens, H., Pakanen, V.M., Jäkäläniemi, A., Tuomi, J., Kvist, L., 2017. Low population viability in small endangered orchid populations: Genetic variation, seedling recruitment and stochasticity. Biological Conservation 210, 174–183. doi:10.1016/j.biocon.2017.04.019.

Hill, W.G., 1972. Effective size of populations with overlapping generations. Theoretical Population Biology 3, 278–289. doi:10.1016/0040-5809(72)90004-4.

Hill, W.G., 1979. A note on effective population size with overlapping generations. Genetics 92, 317–322. doi:10.1093/genetics/92.1.317.

Johnson, D.L., 1977. Inbreeding in populations with overlapping generations. Genetics 87, 581–591. doi:10.1093/genetics/87.3.581.

Jones, O.R., Scheuerlein, A., Salguero-Gómez, R., Camarda, C.G., Schaible, R., Casper, B.B., Dahlgren, J.P., Ehrlén, J., García, M.B., Menges, E.S., Quintana-Ascencio, P.F., Caswell, H., Baudisch, A., Vaupel, J.W., 2014. Diversity of aging across the tree of life. Nature 505, 169–173. doi:10.1038/nature12789.

Kettle, C.J., Hollingsworth, P.M., Jaffre, T., Moran, B., Ennos, R.A., 2007. Identifying the early genetic consequences of habitat degradation in a highly threatened tropical conifer, *Araucaria nemorosa* Laubenfels. Molecular Ecology 16, 3581–3591. doi:10.1111/j.1365-294X.2007.03419.x.

Knight, T.M., 2004. The effects of herbivory and pollen limitation on a declining population of *TRILLIUM GRANDIFLORUM*. Ecological Applications 14, 915–928. doi:10.1890/03-5048.

Knight, T.M., Caswell, H., Kalisz, S., 2009. Population growth rate of a common understory herb decreases non-linearly across a gradient of deer herbivory. Forest Ecology and Management 257, 1095–1103. doi:10.1016/j.foreco.2008.11.018.

Linhart, Y.B., Mitton, J.B., Sturgeon, K.B., Davis, M.L., 1981. Genetic variation in space and time in a population of poderosa pine. Heredity 46, 407–426. doi:10.1038/hdy.1981.49.

Mimura, M., Yahara, T., Faith, D.P., Vázquez-Domínguez, E., Colautti, R.I., Araki, H., Javadi, F., Núñez-Farfán, J., Mori, A.S., Zhou, S., Hollingsworth, P.M., Neaves, L.E., Fukano, Y., Smith, G.F., Sato, Y.I., Tachida, H., Hendry, A.P., 2017. Understanding and monitoring the consequences of human impacts on intraspecific variation. Evolutionary Applications 10, 121–139. doi:10.1111/eva.12436.

Murren, C.J., 2003. Spatial and demographic population genetic structure in *Catasetum viridiflavum* across a human-disturbed habitat. Journal of Evolutionary Biology 16, 333–342. doi:10.1046/j.1420-9101.2003.00517.x.

Ohara, M., Takada, T., Kawano, S., 2001. Demography and reproductive strategies of a polycarpic perennial, *Trillium apetalon* (Trilliaceae). Plant Species Biology 16, 209–217. doi:10.1046/j.1442-1984.2001.00062.x.

Orive, M., 1993. Effective population size in organisms with complex life-histories. Theoretical Population Biology 44, 316–340. doi:10.1006/tpbi.1993.1031.

Ramsayer, J., Kaltz, O., Hochberg, M.E., 2013. Evolutionary rescue in populations of pseudomonas fluorescens across an antibiotic gradient. Evolutionary Applications 6, 608–616. doi:10.1111/eva.12046.

Schmidt, D.J., Fallon, S., Roberts, D.T., Espinoza, T., McDougall, A., Brooks, S.G., Kind, P.K., Bond, N.R., Kennard, M.J., Hughes, J.M., 2018. Monitoring age-related trends in genomic diversity of Australian lungfish. Molecular Ecology 27, 3231–3241. doi:10.1111/mec.14791.

Shea, K., Kelly, D., 1998. Estimating biocontrol agent impact with matrix models: *Carduus nutans* in New Zealand. Ecological Applications 8, 824–832. doi:10.1890/1051-0761(1998)008[0824:EBAIWM]2.0.CO;2.

Silvertown, J., 1987. Introduction to Plant Population Ecology. 2 ed., Longman Scientific & Technical.

Tomimatsu, H., Ohara, M., 2010. Demographic response of plant populations to habitat fragmentation and temporal environmental variability. Oecologia 162, 903–911. doi:10.1007/s00442-009-1505-8.

Torices, R., Méndez, M., Gómez, J.M., 2011. Where do monomorphic sexual systems fit in the evolution of dioecy? insights from the largest family of angiosperms. New Phytologist 190, 234–248. doi:10.1111/j.1469-8137.2010.03609.x.

559 Vranckx, G., Jacquemyn, H., Mergeay, J., Cox, K., Kint, V., Muys, B., Hon-
560 nay, O., 2014. Transmission of genetic variation from the adult generation
561 to naturally established seedling cohorts in small forest stands of peduncu-
562 late oak (*Quercus robur* L.). Forest Ecology and Management 312, 19–27.
563 doi:10.1016/j.foreco.2013.10.027.

564 Waples, R.S., Do, C., Chopelet, J., 2011. Calculating N_e and N_e/N in age-
565 structured populations: a hybrid Felsenstein-Hill approach. Ecology 92,
566 1513–1522.

567 Waples, R.S., Luikart, G., Faulkner, J.R., Tallmon, D.A., 2013. Simple
568 life-history traits explain key effective population size ratios across di-
569 verse taxa. Proceedings of the Royal Society B: Biological Sciences 280,
570 20131339. doi:10.1098/rspb.2013.1339.

571 Yonezawa, K., Kinoshita, E., Watano, Y., Zentoh, H., 2000. Formulation and
572 estimation of the effective size of stage-structured populations in *Fritillaria*
573 *camtschatcensis*, a perennial herb with a complex life history. Evolution
574 54, 2007–2013. doi:10.1111/j.0014-3820.2000.tb01244.x.

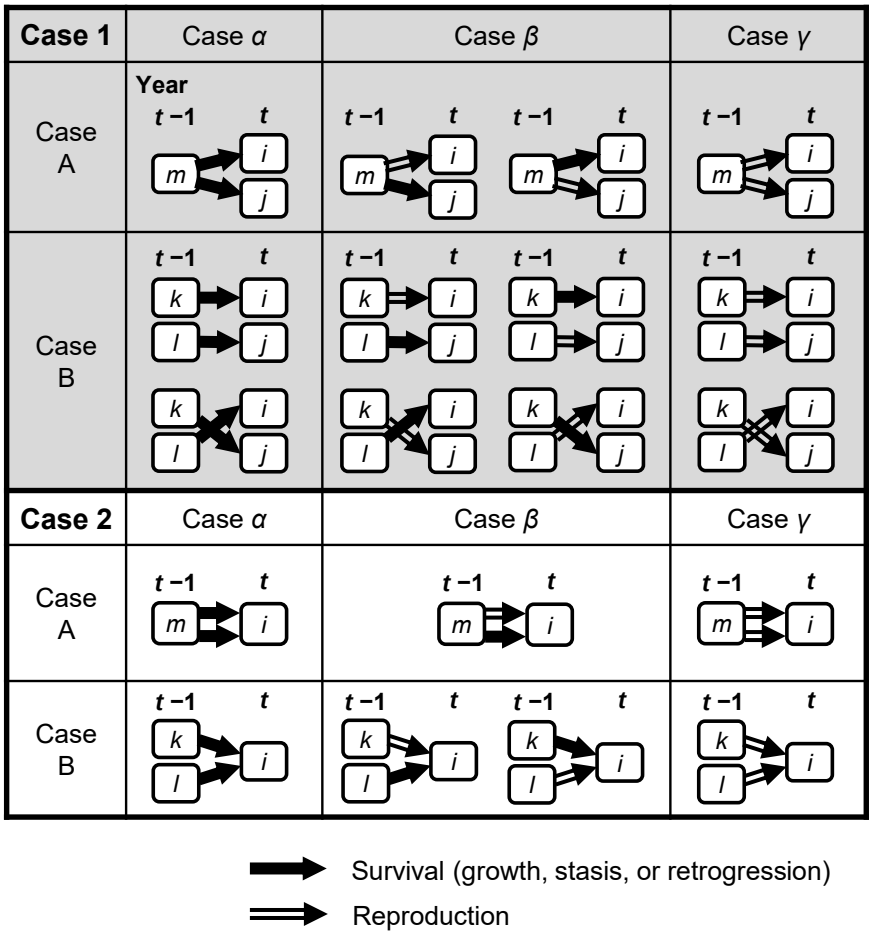

Figure 1: Temporal trajectories from time $t-1$ to t with regard to the two genes sampled in time t. Rounded rectangles stand for life history stages. Arrows stand for the temporal movements of genes either by survival (single line) or reproduction (double line). There are 12 mutually exclusive situations based on three criteria: (1) whether the destinations are different (case 1, shown on gray background) or not (case 2, shown on white); (2) whether the origins are the same (case A) or not (case B); (3) how the two genes were transferred (case α: survival; case β: survival and reproduction; case γ: reproduction)

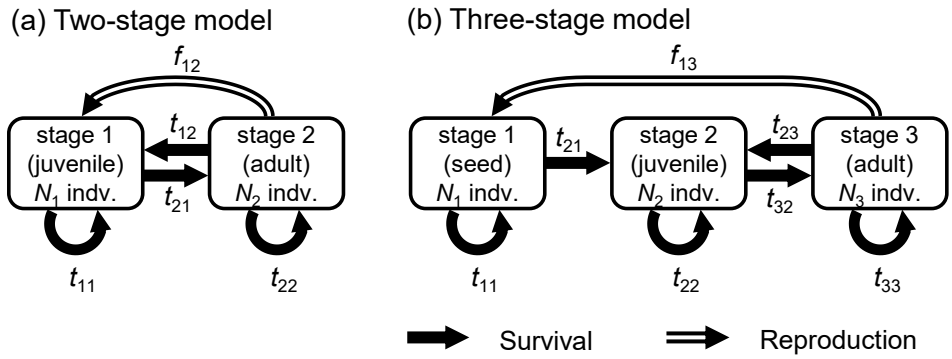

Figure 2: The two model used in analysis: (a) two-stage model and (b) three stage model. Arrows represent flow of individuals, or genes, either by survival (single line) or reproduction (double line)

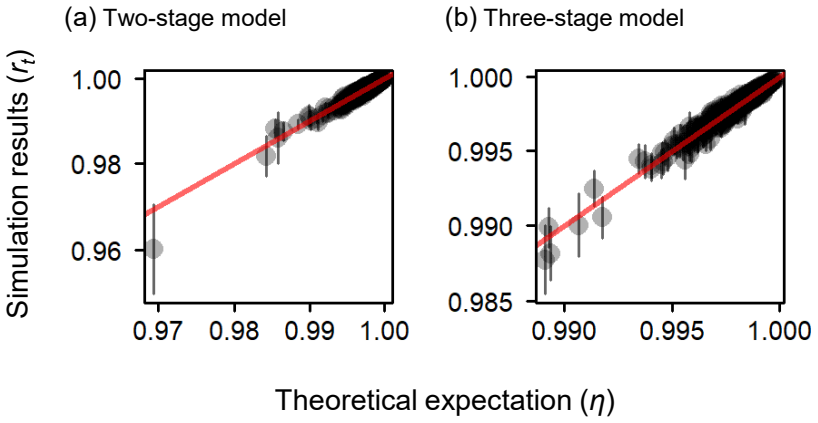

Figure 3: Comparison between the theoretical expectation of the annual change rate of the probability of non-identical-by-descent (η) and the simulation results of that of expected heterozygosity (r_t) for (a) the two-stage and (b) the three-stage model when $N = 100$. Each gray semi-transparent point corresponds to one of the 500 parameter sets. As for r_t, geometric mean over $1 \leq t \leq 200$ is shown with standard error (vertical bar). Red lines represent $\eta = r_t$

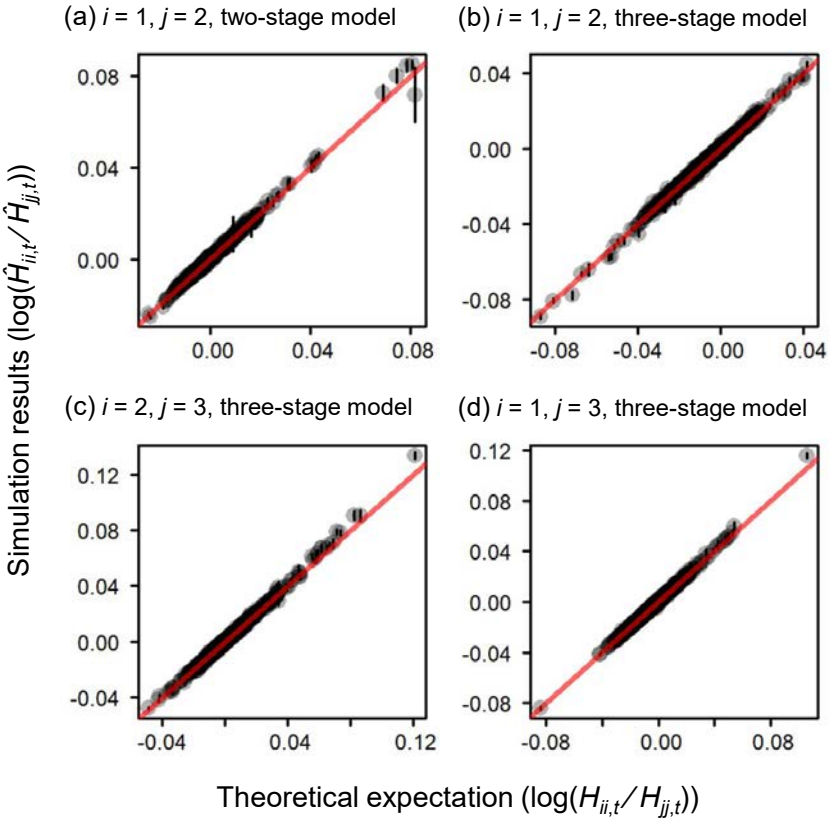

Figure 4: Comparison of demographic genetic structure between the theoretical expectations ($\log(H_{ii,t}/H_{jj,t})$) and the simulation results ($\log(\hat{H}_{ii,t}/\hat{H}_{jj,t})$) when $N = 100$. Each gray semi-transparent point corresponds to one of the 500 parameter sets. As for the simulation results, mean and standard error (vertical bar) over $1 \leq t \leq 200$ are shown. There is one proxy for the two-stage model (a: $i = 1$ and $j = 2$), while there are three proxies for the three-stage model (b: $i = 1$ and $j = 2$; c: $i = 2$ and $j = 3$; d: $i = 1$ and $j = 3$). The theoretical expectations exactly match with the simulation results when plotted on the red lines

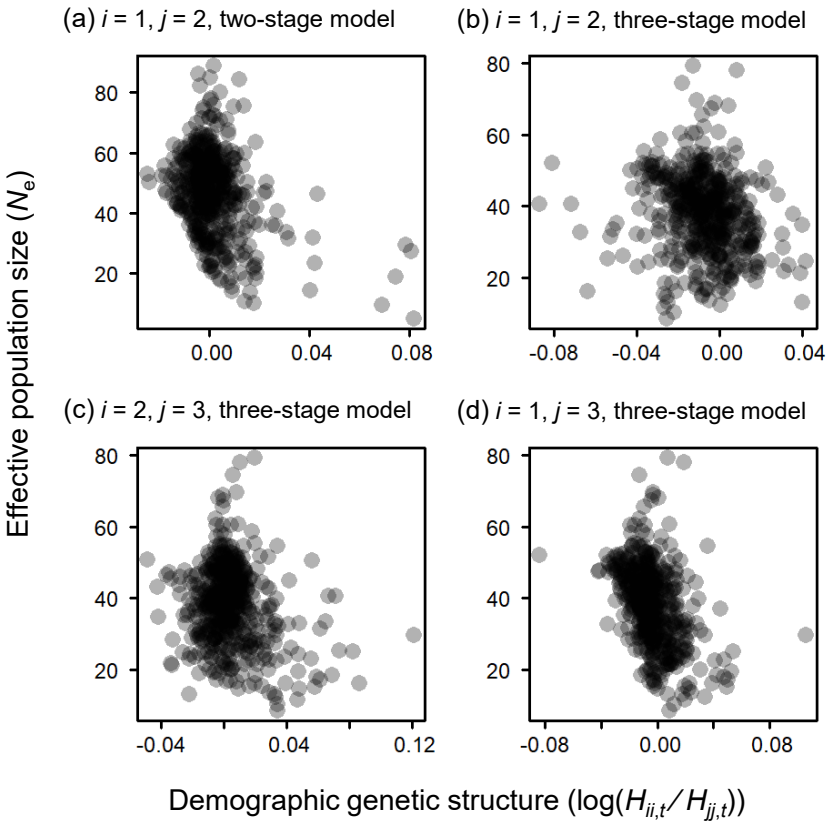

Figure 5: Comparison of demographic genetic structure ($\log(H_{ii,t}/H_{jj,t})$) with effective population size (N_e) when $N = 100$. (a) $i = 1$ and $j = 2$ of the two-stage model, (b) $i = 1$ and $j = 2$, (c) $i = 2$ and $j = 3$, (d) $i = 1$ and $j = 3$ of the three-stage model

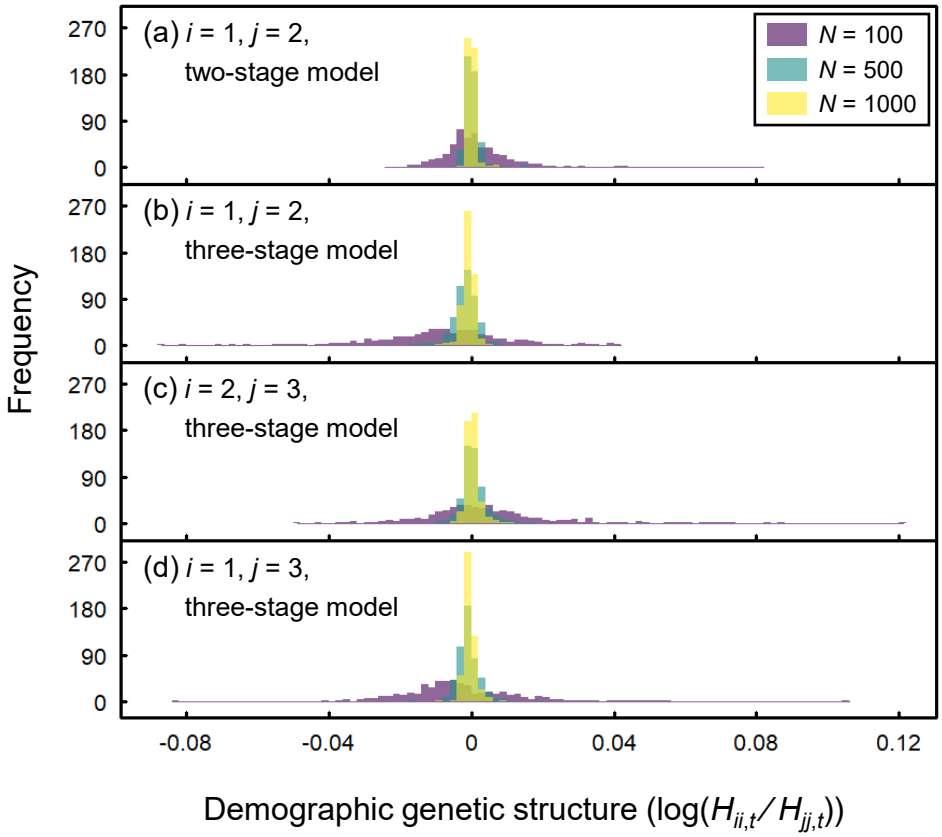

Figure 6: Histogram of demographic genetic structure ($\log(H_{ii,t}/H_{jj,t})$) with varying N. (a) $\log(H_{11,t}/H_{22,t})$ of the two-stage model, (b) $\log(H_{11,t}/H_{22,t})$, (c) $\log(H_{22,t}/H_{33,t})$, (d) $\log(H_{11,t}/H_{33,t})$ of the three-stage model

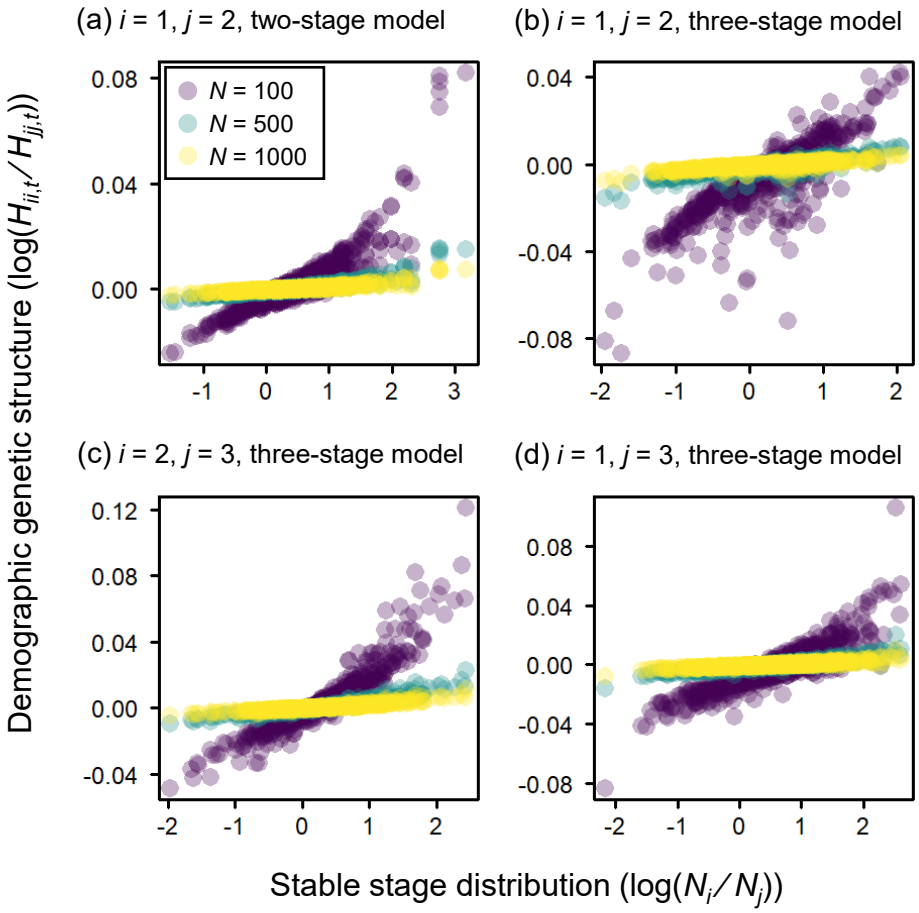

Figure 7: Relationships between stable stage distribution ($\log(N_i/N_j)$) and demographic genetic structure ($\log(H_{ii,t}/H_{jj,t})$) with varying N.

Corrigendum

Corrigendum to ‘Modeling temporal dynamics of genetic diversity in stage-structured plant populations with reference to demographic genetic structure’
[Theoretical Population Biology 148 (2022) 76-85]

Yoichi Tsuzuki[a], Takenori Takada[a], Masashi Ohara[a]
[a]Graduate School of Environmental Science, Hokkaido University, N10W5, Sapporo City, 060-0810, Hokkaido Prefecture, Japan

---

The authors regret that there are typographical errors in the summation operators in Eqs. (5), (6), (8), and (9). In analogous to the age-structured model of Felsenstein (1971), $H_{ij,t}$ (or $H_{kl,t}$) could be also written as $H_{ji,t}$ (or $H_{lk,t}$). Although we consistently used $H_{ij,t}$ ($i \le j$) when deriving the matrix equation to avoid the redundant notation, as in Eqs. (20) and (21), we mistakenly wrote the range of i and j of the two successive summation operators in the fourth to sixth lines of Eq. (5), the second line of Eq. (6), the fourth to sixth lines of Eq. (8), and the third line of Eq. (9). We corrected these lines to avoid duplicate summations for the same two stages as follows.

$$
\begin{aligned}
H_{ij,t|1\cap A\cap\alpha} &= \sum_{m=1}^{n}\left\{\frac{t_{im}t_{jm}N_m^2}{N_iN_j}\times\frac{1}{1-1/(2N_m)}H_{mm,t-1}\right\}\\
H_{ij,t|1\cap A\cap\beta} &= \sum_{m=1}^{n}\left\{\frac{(t_{im}f_{jm}+f_{im}t_{jm})N_m^2}{N_iN_j}\times H_{mm,t-1}\right\}\\
H_{ij,t|1\cap A\cap\gamma} &= \sum_{m=1}^{n}\left(\frac{f_{im}f_{jm}N_m^2}{N_iN_j}\times H_{mm,t-1}\right)\\
H_{ij,t|1\cap B\cap\alpha} &= \sum_{k=1}^{n-1}\sum_{l=k+1}^{n}\left\{\frac{(t_{ik}t_{jl}+t_{il}t_{jk})N_kN_l}{N_iN_j}\times H_{kl,t-1}\right\}\\
H_{ij,t|1\cap B\cap\beta} &= \sum_{k=1}^{n-1}\sum_{l=k+1}^{n}\left\{\frac{(t_{ik}f_{jl}+f_{ik}t_{jl}+t_{il}f_{jk}+f_{il}t_{jk})N_kN_l}{N_iN_j}\times H_{kl,t-1}\right\}\\
H_{ij,t|1\cap B\cap\gamma} &= \sum_{k=1}^{n-1}\sum_{l=k+1}^{n}\left\{\frac{(f_{ik}f_{jl}+f_{il}f_{jk})N_kN_l}{N_iN_j}\times H_{kl,t-1}\right\}.
\end{aligned}
\tag{5}
$$

$$
\begin{aligned}
H_{ij,t} = \sum_{m-1}^{n}\frac{N_m^2}{N_iN_j}\left\{\frac{t_{im}t_{jm}}{1-1/(2N_m)}+f_{im}t_{jm}+t_{im}f_{jm}+f_{im}f_{jm}\right\}H_{mm,t-1}\\
+\sum_{k=1}^{n-1}\sum_{l=k+1}^{n}\frac{N_kN_l}{N_iN_j}(a_{ik}a_{jl}+a_{il}a_{jk})H_{kl,t-1}.
\end{aligned}
\tag{6}
$$

$$
\begin{aligned}
H_{ii,t|2\cap A\cap\alpha} &= \sum_{m=1}^{n}\left\{\left(\frac{t_{im}N_m}{N_i}\right)^2\times\frac{1-1/(2t_{im}N_m)}{1-1/(2N_m)}H_{mm,t-1}\right\}\\
H_{ii,t|2\cap A\cap\beta} &= \sum_{m=1}^{n}\left(\frac{2t_{im}f_{im}N_m^2}{N_i^2}\times H_{mm,t-1}\right)\\
H_{ii,t|2\cap A\cap\gamma} &= \sum_{m=1}^{n}\left\{\left(\frac{f_{im}N_m}{N_i}\right)^2\times\left(1-\frac{1}{2f_{im}N_m}\right)H_{mm,t-1}\right\}\\
H_{ii,t|2\cap B\cap\alpha} &= \sum_{k=1}^{n-1}\sum_{l=k+1}^{n}\left(\frac{2t_{ik}t_{il}N_kN_l}{N_i^2}\times H_{kl,t-1}\right)\\
H_{ii,t|2\cap B\cap\beta} &= \sum_{k=1}^{n-1}\sum_{l=k+1}^{n}\left\{\frac{2(t_{ik}f_{il}+f_{ik}t_{il})N_kN_l}{N_i^2}\times H_{kl,t-1}\right\}\\
H_{ii,t|2\cap B\cap\gamma} &= \sum_{k=1}^{n-1}\sum_{l=k+1}^{n}\left(\frac{2f_{ik}f_{il}N_kN_l}{N_i^2}\times H_{kl,t-1}\right).
\end{aligned}
\tag{8}
$$

$$
\begin{aligned}
H_{ii,t} = \sum_{m-1}^{n}\Bigg\{&\left(\frac{t_{im}N_m}{N_i}\right)^2\frac{1-1/(2t_{im}N_m)}{1-1/(2N_m)}+\frac{2t_{im}f_{im}N_m^2}{N_i^2}\\
&+\left(\frac{f_{im}N_m}{N_i}\right)^2\left(1-\frac{1}{2f_{im}N_m}\right)\Bigg\}H_{mm,t-1}\\
&+\sum_{k=1}^{n-1}\sum_{l=k+1}^{n}\frac{2a_{ik}a_{il}N_kN_l}{N_i^2}H_{kl,t-1}.
\end{aligned}
\tag{9}
$$

The same correction applies to the two successive summation operators in Eqs. S15-S18, S23-S25, and S31-32 in the Supporting Information. The analytical results in the original paper are not impacted by the error because the results were obtained based on the correct equations shown in this corrigendum.

The authors would like to apologise for any inconvenience caused.

DOI of original article: 10.1016/j.tpb.2022.11.001
Corresponding author
Yoichi Tsuzuki
Graduate School of Environmental Science, Hokkaido University, N10W5, Sapporo City, 060-0810, Hokkaido Prefecture, Japan
yoichi.tsuzuki.95@gmail.com